JOURNAL OF GEOPHYSICAL RESEARCH, VOL. 105, NO. B7, PAGES 16,271–16,277, JULY 10, 2000

A new assessment of long-wavelength gravitational variations

J. L. Chen
Center for Space Research, University of Texas at Austin

C. R. Wilson[1]
Department of Geological Sciences, University of Texas at Austin

R. J. Eanes and B. D. Tapley
Center for Space Research, University of Texas at Austin

Abstract. We estimate the degree 2 long-wavelength gravitational variations C_{21}, S_{21}, and C_{20} using Earth rotational changes, caused by mass redistribution and movement within the Earth system. These rotation changes are accurately measured by space geodetic techniques. Wind and oceanic current effects are removed from the Earth rotation series using atmospheric and oceanic circulation data-assimilating models. The results are compared with LAGEOS Satellite Laser Ranging (SLR) determinations and also with geophysical contributions estimated from atmospheric surface pressure, continental water storage, and nonsteric sea level changes. Our conjecture is that using Earth rotational changes to infer long-wavelength gravitational variations has the potential to be more accurate than satellite-based techniques in some cases. Consistent with this, we find that C_{21} and S_{21} variations from this study are in better agreement with geophysical observations than LAGEOS SLR determinations of C_{21} and S_{21}. However, the Earth rotation-derived estimate of C_{20} variation is probably less accurate than the LAGEOS-derived result owing to the large atmospheric wind contribution to length-of-day variation which must first be removed and the natural sensitivity of LAGEOS to C_{20} changes via precession of the satellite node.

1. Introduction

Earth rotational variations, including polar motion and length-of-day (LOD) variations, are introduced by mass redistribution and movement within the Earth system and angular momentum exchange between the solid Earth and the atmosphere, oceans, and hydrosphere. Excitations of polar motion and LOD changes due to air and water consist of two kinds of contributions. One is from surface mass load variations due to changes of atmospheric surface pressure, continental water storage, and ocean bottom pressure, and the other is from horizontal surface stress changes (torques) associated with angular momentum exchange between the solid Earth and the surrounding fluids, e.g., wind and ocean current variations.

[1]Also at NASA Headquarters, Washington, D. C.

Paper number 2000JB900115.
0148-0227/00/2000JB900115$09.00

Earth rotational theory (i.e., the Liouville equation) indicates that excitation of polar motion (X, Y) and LOD due to surface mass load variations is proportional to spherical harmonic degree 2 gravitational changes [*Lambeck*, 1980; *Barnes et al.*, 1983; *Eubanks*, 1993], as

$$\begin{aligned} \psi^X_{\text{mass}} &= -1.098 \frac{M_E R_E^2}{C-A} C_{21}, \\ \psi^Y_{\text{mass}} &= -1.098 \frac{M_E R_E^2}{C-A} S_{21}, \\ \psi^{\text{LOD}}_{\text{mass}} &= -0.755 \frac{2 M_E R_E^2}{3C} C_{20}, \end{aligned} \tag{1}$$

where, ψ^X_{mass}, ψ^Y_{mass}, and $\psi^{\text{LOD}}_{\text{mass}}$ are the excitations (due to mass redistribution) of X, Y, and LOD, respectively [*Lambeck*, 1980]. M_E and R_E are the mass and mean radius, and C and A are the two principal inertia moments of the Earth. C_{21}, S_{21}, and C_{20} are the degree 2 order 1 and zonal Stokes coefficients, representing three of the five degree 2 gravitational variations. Elastic deformational effects are included in the above equations in the numerical factors 1.098 and 0.755, assuming that the core does not participate in the Earth rotational changes at seasonal or shorter periods [*Barnes et al.*, 1983; *Eubanks*, 1993].

This relationship provides a means to infer long-wavelength gravitational variations from accurately determined Earth rotational changes, provided that we can effectively estimate and subtract excitations due to winds and ocean currents. It also provides an opportunity to compare LAGEOS satellite laser ranging (SLR) determination of gravitational changes with those estimated from Earth rotational variations. In addition, the Earth rotation-derived results may strengthen gravity field solution from the future Gravity Recovery And Climate Experiment (GRACE) mission, supplementing the LAGEOS SLR measurements. Another significance of this approach is that it will provide a chance to detect high-frequency (e.g., submonthly) variations in the degree 2 gravity fields, which are not detectable from either LAGEOS SLR data [*Eanes et al.*, 1997] or the GRACE observation (with a repeat cycle of 2-3 weeks) [*Tapley and Reigber*, 1998].

In this paper, we estimate C_{21}, S_{21}, and C_{20} variations using polar motion (X, Y) and LOD variations determined by modern space geodetic techniques, including very long baseline interferometry (VLBI), Global Positioning System (GPS), SLR, and lunar laser ranging (LLR). Atmospheric wind excitations are removed from observed X, Y, and LOD excitations using atmospheric angular momentum (AAM) estimates by *Salstein and Rosen* [1997] based on the National Centers for Environmental Prediction (NCEP) atmospheric assimilation reanalysis system. Excitations from ocean currents are subtracted from X, Y, and LOD observations using results by *Johnson et al.* [1999] based on the Parallel Ocean Climate Model (POCM) [D. Stammer et al., unpublished manuscript, 1998]. These geodetic estimates are compared with predicted C_{21}, S_{21}, and C_{20} changes derived from assimilated atmospheric and hydrological models and TOPEX/Poseidon satellite radar altimeter observation.

2. Data and Computations

2.1. Excitations of X, Y, and LOD

The X, Y, and LOD time series are from SPACE97 [*Gross*, 1996], which is obtained from various space geodetic observations (VLBI, GPS, SLR, and LLR) through a Kalman filter combination [*Eubanks*, 1988]. The data cover the period September 1976 through January 1998, with daily temporal sampling. Tidal corrections have been removed from the time series.

The observed excitations of X and Y are conventionally estimated on the basis of following discrete linear polar motion filter developed by *Wilson* [1985]:

$$\Psi_t = \frac{i \exp -i\pi F_c T}{\sigma_c T}[m_{t+\frac{T}{2}} - \exp i\sigma_c T m_{t-\frac{T}{2}}], \qquad (2)$$

where, $\Psi = \psi^X + i\psi^Y$ is the complex excitation function of X and Y, $m = X$ -iY is the complex location of the rotation pole in the terrestrial reference system (the negative sign comes from the left-handed coordinate system used in the polar motion data), X and Y are the polar motion series from SPACE97, $\sigma_c = 2\pi F_c(1 + i/2Q)$ is the complex Chandler frequency, F_c is 0.843 cycles/yr, Q is the quality factor, estimated to be 175 [*Wilson and Vicente*, 1990], and T is the sampling interval.

The LOD excitations are simply defined as the normalized (dimensionless) LOD variations as

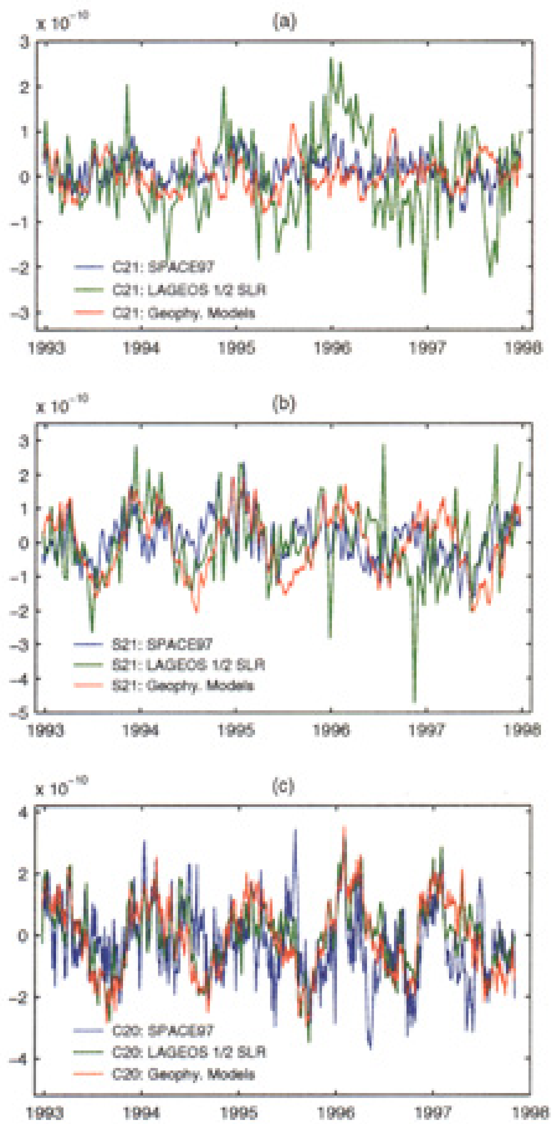

Plate 1. Comparisons of three estimates of the C_{21}, S_{21}, and C_{20} variations based on SPACE97 X, Y, and LOD, LAGEOS 1/2 SLR data, and geophysical models.

$$\psi^{\mathrm{LOD}} = \Delta LOD/\Delta_o, \qquad (3)$$

where ΔLOD is from SPACE97 and Δ_o = 86,400,000 millisecond(ms), the nominal length of the day.

After subtracting wind and ocean current contributions from observed excitations (ψ^X, ψ^Y, and ψ^{LOD}) using NCEP reanalysis AAM [*Salstein and Rosen*, 1997] and POCM results [*Johnson et al.*, 1999], we use the residual excitations (ψ^X_{mass}, ψ^Y_{mass}, and $\psi^{\mathrm{LOD}}_{\mathrm{mass}}$) to estimate C_{21}, S_{21}, and C_{20} variations (called $C_{21}^{\mathrm{SPACE97}}$, $S_{21}^{\mathrm{SPACE97}}$, and $C_{20}^{\mathrm{SPACE97}}$ hereafter) using (1). Wind excitations are computed from the surface to the top of the NCEP reanalysis model, i.e., 10 mb, and the second-order motion terms are neglected [*Barnes et al.*, 1983]. Ocean current excitations are relatively less well determined owing to limitations from model development. Even though wind effects dominate LOD variation, ocean current contribution to LOD is, however, much smaller and only accounts for a few percent of wind excitation [*Johnson et al.*, 1999]. Both winds and ocean currents are not a dominant contributor to polar motion excitation.

2.2. LAGEOS SLR Determination

SLR tracking data of LAGEOS 1 and LAGEOS 2 have been used to determine time series of gravitational field harmonics up to degree 5 [*Eanes et al.*, 1997]. Tracking data from the two satellites are able to isolate the degree two harmonics of the mass distribution from the higher degree harmonics with reasonable accuracy. C_{21}, S_{21}, and C_{20} (called C_{21}^{SLR}, S_{21}^{SLR}, and C_{20}^{SLR} hereafter) time series used in this study span the period October 1992 (when LAGEOS 2 was launched) to October 1998. C_{21}^{SLR} and S_{21}^{SLR} series are sampled about every 12 days, and the C_{20}^{SLR} series is sampled every 3 days. These time series show significant seasonal and intraseasonal variability, which are not well understood because of the lack of independent techniques to confirm them.

Polar motion and the degree 2 order 1 gravitational change (C_{21} and S_{21}) cannot be simultaneously solved using either LAGEOS 1 or LAGEOS 2 alone. However, because polar motion effects on satellite orbital perturbation are dependent on satellite inclination [*Kaula*, 1966], when combining the two satellites' observations, both polar motion and C_{21} and S_{21} can be solved [*Eanes et al.*, 1997].

2.3. Geophysical Model Predictions

In addition to the Earth rotational observations and LAGEOS SLR tracking data, the C_{21}, S_{21}, and C_{20} variations are also estimated from mass load variations due to atmospheric pressure, continental water storage, and nonsteric sea level changes (called $C_{21}^{\mathrm{Geophy.}}$, $S_{21}^{\mathrm{Geophy.}}$, and $C_{20}^{\mathrm{Geophy.}}$ hereafter). The atmospheric data are from the NCEP reanalysis [*Kalnay et al.*, 1996] surface pressure field, with 6-hourly time sample and a 2.5° x 2.5° spatial resolution for the period January 1973 to April 1998. Continental water storage changes are estimated from the soil moisture and snow fields from NCEP Climate Data Assimilation System 1 (CDAS-1) [*Kalnay et al.*, 1996]. The soil moisture and snow data are given monthly on a Gaussian grid spanning the period January 1958 to September 1998. The soil moisture estimates are for two layers, surface to 10 cm depth and 10-200 cm depth.

Oceanic contributions are computed from nonsteric sea level changes using TOPEX/Poseidon satellite altimeter data and a steric sea surface height model [*Chen et al.*, 2000]. The TOPEX/Poseidon sea sur-

Table 1. The Amplitude and Phase of Annual and Semiannual Variations of C_{21}, S_{21}, and C_{20} Estimated Using the Least Squared Fit for the Results Derived from SPACE97 X, Y, and LOD Time Series, LAGEOS 1/2 SLR Tracking Data, and Geophysical Models

	Sources	Annual		Semiannual	
		Amp ($\times 10^{-10}$)	Phase, deg	Amp ($\times 10^{-10}$)	Phase, deg
C_{21}	SPACE97	0.20	125	0.12	98
C_{21}	LAGEOS 1/2 SLR	0.35	59	0.17	160
C_{21}	Geophysical Models	0.25	192	0.31	33
S_{21}	SPACE97	0.50	125	0.23	265
S_{21}	LAGEOS 1/2 SLR	0.53	65	0.15	206
S_{21}	Geophysical Models	1.2	68	0.23	234
C_{20}	SPACE97	0.37	54	0.80	54
C_{20}	LAGEOS 1/2 SLR	1.1	35	0.40	130
C_{20}	Geophysical Models	1.5	43	0.22	108

The phase ϕ is defined as $\sin(2\pi f t + \phi)$, and the epoch t is referred to January 1, 0000 UT.

face anomaly data include cycles 10 - 221 (December 1992 to September 1998, 10-day repeat cycle) and are averaged into a 1° x 1° grid [*Tapley et al.*, 1994]. The $C_{21}^{\text{Geophy.}}$, $S_{21}^{\text{Geophy.}}$, and $C_{20}^{\text{Geophy.}}$ are computed using a very similar approach described by *Chen et al.* [1999]. An inverted barometer (IB) correction, assuming a constant reference sea surface pressure, has been applied to both atmospheric surface pressure data and TOPEX/Poseidon data [*Callahan*, 1993].

3. Result and Comparison

3.1. Seasonal Variability

C_{21}^{SPACE97}, S_{21}^{SPACE97}, and C_{20}^{SPACE97} variations estimated from observed X, Y, and LOD excitations are shown by blue curves in Plate 1a, 1b, and 1c, respectively, superimposed by corresponding estimates from LAGEOS SLR tracking data (shown by green curves) and geophysical models (shown by red curves). A 12-day moving average filter was applied to C_{21}^{SPACE97}, S_{21}^{SPACE97}, $C_{21}^{\text{Geophy.}}$, and $S_{21}^{\text{Geophy.}}$ series, and a 3-day moving average filter was applied to C_{20}^{SPACE97} and $C_{20}^{\text{Geophy.}}$ series. This gives them approximately the same bandwidth as the C_{21}^{SLR} and S_{21}^{SLR} estimates that sampled every 12 days and the C_{20}^{SLR} series sampled every 3 days. The amplitude and phase of annual and semiannual variations of C_{21}, S_{21}, and C_{20} are estimated by the least squares and listed in Table 1.

Some reasonable agreements appear among the estimates from three different approaches at a broad band of frequencies, especially among the seasonal variations of S_{21} and C_{20}. The C_{21} variations show a relatively poorer agreement with each other (see Table 1), which is likely due to the weaker seasonal variability of C_{21} (30-50% of those of C_{20} and S_{21}). The relatively weaker C_{21} variations, corresponding to the mass-induced excitations of polar motion X, are generally attributed to the geographic distribution of the continents, which are more close to the Y axis. Therefore the S_{21} variations (or Y excitations) are relatively more sensitive to the strong seasonal variations over the continents, including atmospheric surface pressure and continental water storage changes. The pressure variations over the oceans are more or less canceled out by the IB effects, although the mechanism of IB effects are still not completely understood.

The strong seasonal variability in the zonal C_{20} variations is due to the well-known large-scale zonal patterns in atmospheric, oceanic, and hydrologic general circulation systems. The C_{20}^{SLR} estimate agrees better with the geophysical model predictions in both amplitudes and phases compared to the LOD-derived results (Table 1). The better performance of LAGEOS SLR tracking data in determining the degree 2 zonal term, i.e., C_{20}, is not surprising. This is because, first, the C_{20} (also commonly expressed as J2 by a scale factor) variations are the best determined gravitational changes by LAGEOS SLR data [e.g., *Yoder et al.*, 1983; *Gutierrez and Wilson*, 1987; *Cheng et al.*, 1989; *Nerem et al.*, 1993; *Gegout and Cazenave*, 1993; *Chao and Eanes*, 1995; *Dong et al.*, 1996;] owing to the natural sensitivity of LAGEOS to C_{20} changes via precession of the satellite node, and second, the wind effects are very dominant in driving LOD variations and must first be removed from the observed LOD variations. The latter makes the C_{20} estimates less accurate than the LAGEOS SLR determinations. Therefore the C_{20}^{SLR} should be more accurate and preferred.

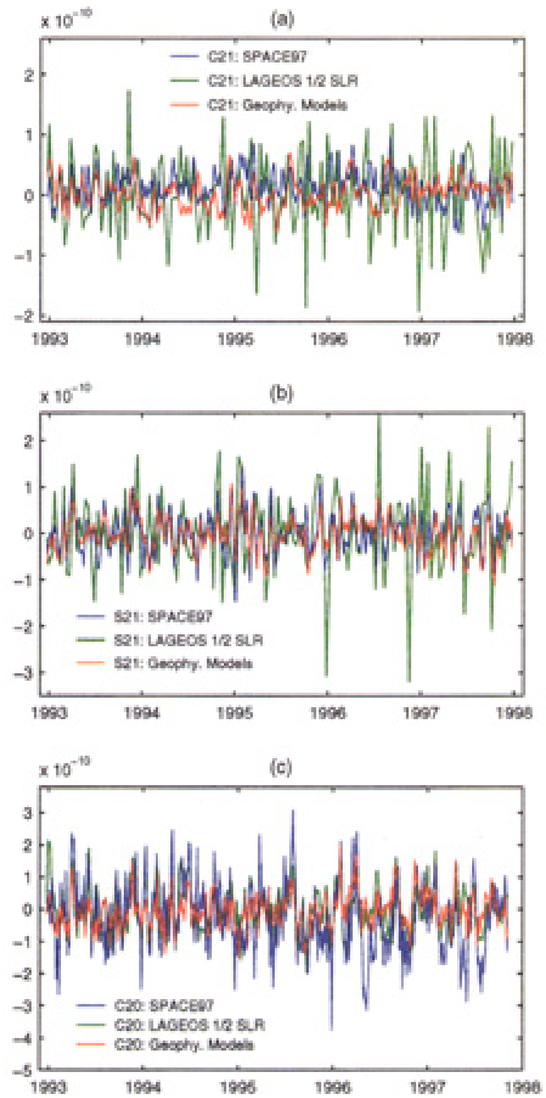

Plate 2. The comparisons of intraseasonal C_{21}, S_{21}, and C_{20} variations based on SPACE97 X, Y, and LOD, LAGEOS 1/2 SLR data, and geophysical models. Annual and semiannual (or longer periods) variations are removed from all time series.

3.2. Intraseasonal Variability

Nonseasonal variations are shown in Plate 2 after annual and semiannual variations in Table 1 are subtracted from all time series. Visual inspection of Plate 2 suggests some degree of correlation among the series. Figure 1 shows cross correlations between the SPACE97 estimates and geophysical model predictions and also between the LAGEOS SLR solutions and geophysical model predictions for intraseasonal C_{21}, S_{21}, and C_{20} variations. The peak correlation coefficients at zero phase lag are estimated from the cross-correlation time series and listed in Table 2.

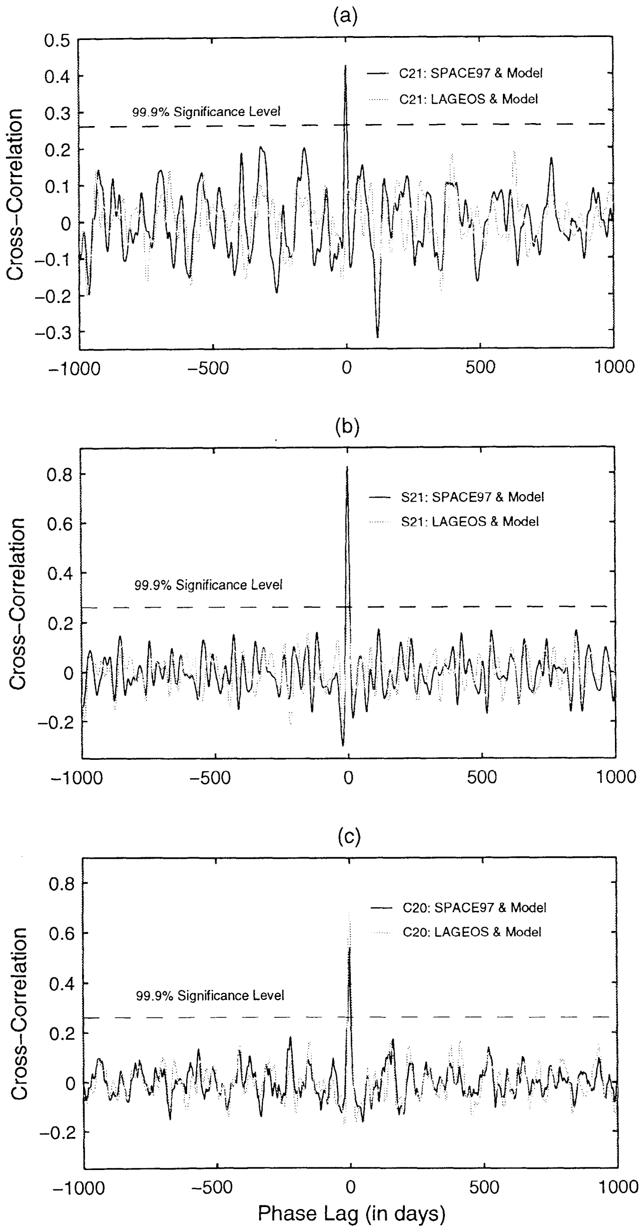

Figure 1. Cross-correlation analysis for intraseasonal C_{21}, S_{21}, and C_{20} variations between SPACE97 estimates and geophysical model predictions (solid curves) and also between LAGEOS 1/2 SLR solutions and geophysical model predictions (dashed curves) in units of decibel (dB).

It is quite evident from Plate 2 and Table 2 that there is strong peak (a correlation coefficient estimate of 0.42) at zero phase lag between $C_{21}^{\mathrm{SPACE97}}$ and $C_{21}^{\mathrm{Geophy.}}$, while there is no notable peak between C_{21}^{SLR} and $C_{21}^{\mathrm{Geophy.}}$. The peak correlation coefficient between $S_{21}^{\mathrm{SPACE97}}$ and $S_{21}^{\mathrm{Geophy.}}$ is as large as 0.82 compared with the peak value 0.28 between S_{21}^{SLR} and $S_{21}^{\mathrm{Geophy.}}$. Both $C_{20}^{\mathrm{SPACE97}}$ and C_{20}^{SLR} are strongly correlated with $C_{20}^{\mathrm{Geophy.}}$ (see Plate 2 and Table 2). However, C_{20}^{SLR} has a larger peak correlation coefficient (0.69) than that of $C_{20}^{\mathrm{SPACE97}}$ (0.54), indicating a consistent better performance of LAGEOS SLR tracking data in determining the C_{20} variations at both seasonal and intraseasonal timescales.

3.3. Power Spectral Analysis

We compute power spectral density of the three kinds of estimates of C_{21}, S_{21}, and C_{20} using Welch's averaged periodogram method with the results in Figure 2a, 2b, and 2c, respectively. Power spectral comparisons, again, indicate that the $C_{21}^{\mathrm{SPACE97}}$ and $S_{21}^{\mathrm{SPACE97}}$ estimates are in considerably better agreement with geophysical model predictions in most of the frequencies we examined (from annual or 1 cycle/yr to 15 cycles/yr; see Figure 2). The C_{21}^{SLR} and $S_{21}^{\mathrm{Geophy.}}$ estimates show higher annual amplitudes (Figure 2a and 2b) than the others, as indicated in Table 1. The C_{20}^{SLR} estimate yields more similar power spectral features to $C_{20}^{\mathrm{Geophy.}}$ (Figure 2c), which is consistent with what we have seen from the above cross-correlation analysis.

4. Discussion

This study is a new attempt to estimate the degree 2 gravitational variations C_{21}, S_{21}, and C_{20} using the Earth rotational observations, provided that the wind and ocean current excitations can be effectively modeled and removed from the observed X, Y, and LOD observations. This approach provides an independent means to study these long-wavelength gravitational variations, in addition to LAGEOS (or multisatellite) SLR tracking and geophysical modeling, and takes the advantages of the accurately determined X, Y, and LOD variations and the dense sampling rate of these time series. The results from this study indicate that polar motion X and Y have the potentials to be more accurate than LAGEOS SLR tracking in determining C_{21} and S_{21} variations, especially at intraseasonal timescales. The LAGEOS SLR tracking has been demonstrated to be more reliable than the LOD measurements in deriving the degree 2 zonal C_{20} variations.

The results and conclusions of this study may be affected by many effects. The first and also the most important one is the modeling of wind and ocean current excitations. Although the atmospheric wind effects are fairly well understood and modeled in the atmospheric models [*Dickey*, 1993; *Salstein and Rosen*, 1997], the ocean current excitations are not quite well

Table 2. The Peak Correlation Coefficients at Zero Phase Lag Between SPACE97 Estimates and Geophysical Model Predictions and Between LAGEOS SLR Solution and Geophysical Model Predictions

Sources	C_{21}	S_{21}	C_{20}
SPACE97-Geophy.	0.42	0.82	0.54
SLR-Geophy.	0.09	0.28	0.69

understood because of the relatively less observational constraints in ocean general circulation models [*Semtner and Chervin*, 1992; D. Stammer et al., unpublished manuscript, 1998]. However, because ocean currents are not a significant contributor to X, Y, and LOD excitations [*Marcus et al.*, 1998; *Johnson et al.*, 1999], the errors introduced by using POCM ocean current excitations should be relatively small. This assumption is supported by the good agreements between SPACE97-derived C_{21} and S_{21} variations and geophysical model predictions.

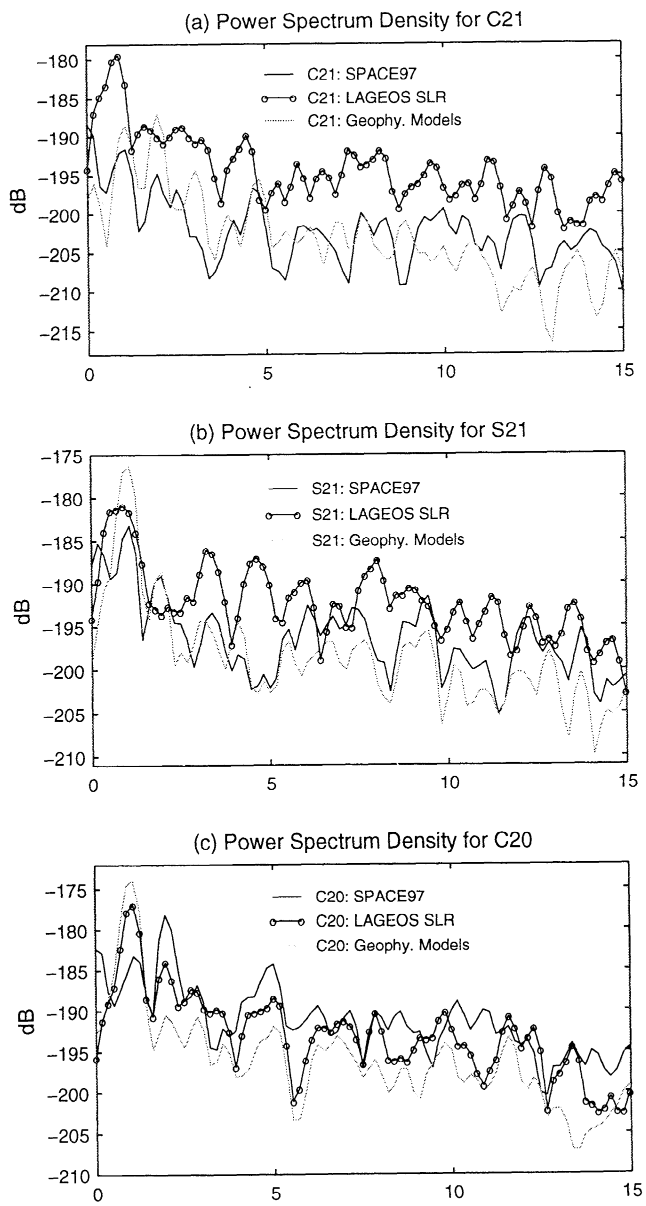

Figure 2. Power spectral density for (a) C_{21}, (b) S_{21}, and (c) C_{20} variations estimated from SPACE97 (solid curves), LAGEOS 1/2 SLR (solid curves with circles), and geophysical models (dashed curves).

Despite the good agreements and correlations for particular frequencies and terms some discrepancies are obvious between the three independent estimates of C_{21}, S_{21}, and C_{20} variations, especially at seasonal timescales. Any of these three estimates, SPACE97 estimates, LAGEOS SLR solutions, and geophysical model predictions could be responsible for the discrepancies. However, the LAGEOS SLR solutions and geophysical model predictions may be a bigger contributor for the errors in C_{21} and S_{21} variations, especially the geophysical model predictions. Except for atmospheric surface pressure contributions, the continental water and oceanic mass redistributions are all among the least known processes in the Earth system. The major discrepancy in C_{20} estimates is that the LOD-derived seasonal amplitude is too small (0.4×10^{-10}) compared to the LAGEOS SLR solution (1.1×10^{-10}) and geophysical model prediction (1.5×10^{-10}), even though the phases agree quite well (see Table 1). This is more likely due to the LOD estimates because of the difficulties in removing the strong and dominant wind effects in LOD variations.

A better estimation of these geodetic quantities may rely on the improvements of LAGEOS (or other satellites) SLR techniques and also on the improvements of geophysical modeling of the atmosphere, hydrosphere, and oceans, especially the outputs from some new data-assimilating systems for the hydrosphere and the oceans, e.g., a new ocean general circulation model assimilating TOPEX/Poseidon satellite altimeter data. Another vital opportunity, which will dramatically improve our knowledge of these gravitational changes, is the observations from future gravity missions, e.g. GRACE, which will lead to revolutionary improvements on modeling mass redistribution and movement in atmospheric, hydrologic, and oceanic models. However, at very long wavelength (or very low degree) the accuracy of GRACE data is very close to that of the LAGEOS SLR tracking data [*Tapley and Reigber*, 1998]. Therefore the Earth rotational observations and SLR tracking data will still play an important and unique role in determining the very low degree gravitational variations. The three independent estimates of C_{21}, S_{21}, and C_{20} variations provide a means to derive an optimally combined solution of C_{21}, S_{21}, and C_{20} time series in the future, which could be used as a constraint to the GRACE measurements.

Acknowledgments. We are grateful to David Salstein for providing the NCEP AAM results and to Tom Johnson for providing the POCM current excitations. This research was supported by the National Aeronautics and Space Administration under grants NAGW-2615 and NAG5-3129.

References

Barnes, R., R. Hide, A. White, and C. Wilson, Atmospheric angular momentum functions, length-of-day changes and polar motion, *Proc. R. Soc. London, Ser. A, 387*, 31-73, 1983.

Callahan, P.S., TOPEX/Poseidon NASA GDR users handbook, *JPL Rep. D-8590*, rev. C, Jet Propul. Lab., Pasadena, Calif., 1993.

Chao, B.F., and R.J. Eanes, Global gravitational changes due to atmospheric mass redistribution as observed by the LAGEOS nodal residual, *Geophys. J. Int., 122*, 755-764, 1995.

Chen, J.L., C.R. Wilson, R.J. Eanes, and R.S. Nerem, Geophysical interpretation of observed geocenter variations, *J. Geophys. Res., 104*(B2), 2683 - 2690, 1999.

Chen, J.L., C.K. Shum, C.R. Wilson, D.P. Chambers, and B.D. Tapley, Seasonal sea level change from TOPEX/Poseidon observation and thermal contribution, *J. Geod., 73*, 638-647, 2000.

Cheng, M.K., R.J. Eanes, C.K. Shum, B.E. Schutz, and B.D. Tapley, Temporal variations in low degree zonal harmonics from Starlette orbit analysis, *Geophys. Res. Lett., 16*, 393-396, 1989.

Dickey, J.O., Atmospheric excitation of the Earth's rotation: Progress and prospects via space geodesy, in *Contributions of Space Geodesy to Geodynamics: Earth Dynamics, Geodyn. Ser.*, Vol. 24, edited by D. Smith and D. Turcotte, pp. 55-70, AGU Washington, D.C., 1993.

Dong, D., R.S. Gross, and J.O. Dickey, Seasonal variations of the Earth's gravitational field: An analysis of atmospheric pressure, ocean tidal, and surface water excitation, *Geophys. Res. Lett., 23*, 725-728, 1996.

Eanes, R.J., S.V. Bettadapur, and R.S. Nerem, Observations of zonal and non-zonal mass redistribution using satellite laser ranging (abstract), *Eos Trans. AGU, 78*(46), Fall Meet. Suppl., F163, 1997.

Eubanks, T.M., Combined Earth rotation series smoothed by a Kalman filter, in *Bureau International de l'Heure Annual Report for 1987*, pp. D85-D86, Obs. de Paris, Paris, 1988.

Eubanks, T.M., Variations in the orientation of the earth, in *Contributions of Space Geodesy to Geodynamic: Earth Dynamics, Geodyn. Ser.*, vol. 24, edited by D. Smith and D. Turcotte, pp. 1-54, AGU, Washington, D.C., 1993.

Gegout, P., and A. Cazenave, Temporal variations of the Earth gravity field for 1985-1989 derived from LAGEOS, *Geophys. J. Int., 114*, 347-359, 1993.

Gross, R.S., Combinations of Earth orientation measurements: SPACE94, COMB94, and POLE94, *J. Geophys. Res., 101*(B4), 8729-8740, 1996.

Gutierrez, R., and C. R. Wilson, Seasonal air and water mass redistribution effects on LAGEOS and Starlette, *Geophys. Res. Lett., 14*, 929-932, 1987.

Johnson, T.J., C.R. Wilson, and B.F. Chao, Oceanic angular momentum variability estimated from the Parallel Ocean Climate Model, 1988-1998, *J. Geophys. Res., 104*(B11), 25,183-25,195, 1999.

Kalnay, E., et al., The NCEP/NCAR 40-year reanalysis project, *Bull. Am. Meteorol. Soc., 77*, 437-471, 1996.

Kaula, W.M., *Theory of Satellite Geodesy*, Blaisdell, *Press* Waltham, Mass., 1966.

Lambeck, K., *The Earth's Variable Rotation: Geophysical Causes and Consequences*, Cambridge Univ. Press, New York, 1980.

Marcus, S., Y. Chao, J. Dickey, and P. Gegout, Detection and modeling of nontidal oceanic effects on Earth's rotation rate, *Science, 281*, 1656-1659, 1998.

Nerem, R.S., B.F. Chao, A.Y. Au, J.C. Chan, S.M. Klosko, N.K. Pavlis, and R.G. Williamson, Temporal variations of the Earth's gravitational field from satellite laser ranging to LAGEOS, *Geophys. Res. Lett., 20*, 595-598, 1993.

Salstein, D.A., and R.D. Rosen, Global momentum and energy signals from reanalysis systems, paper presented at 7th Conference on Climate Variations, Am. Meteorol. Soc., Boston, Mass., 1997.

Semtner, A.J., and R.M. Chervin, Ocean general circulation from a global eddy-resolving model, *J. Geophys. Res., 97*(C4), 5493–5550, 1992.

Tapley, B.D., and C. Reigber, GRACE: A satellite-to-satellite tracking geopotential mapping mission (abstract), *Eos Trans. AGU, 79*(45), Fall Meet. Suppl., F209, 1998.

Tapley, B.D., D.P. Chambers, C.K. Shum, R.J. Eanes, J.C. Ries, and R.H. Stewart, Accuracy assessment of the large-scale dynamic ocean topography from TOPEX/Poseidon altimetry, *J. Geophys. Res., 99*(C12), 24,605 - 24,617, 1994.

Wilson, C.R., Discrete polar motion equations, *Geophys. J. R. Astron. Soc., 80*, 551-554, 1985.

Wilson, C.R. and R.O. Vicente, Maximum likelihood estimates of polar motion parameters in *Variations in Earth Rotation, Geophys. Monogr. Ser.*, vol. 59, edited by D. D. McCarthy and W. E. Carter, pp. 151-155, AGU, Washington, D.C., 1990.

Yoder, C.F., J.G. Williams, J.O. Dickey, B.E. Schutz, R.J. Eanes, and B.D. Tapley, Secular variation of Earth's gravitational harmonic J coefficient from LAGEOS and nontidal acceleration of Earth rotation, *Nature, 303*, 757-762, 1983.

J.L. Chen, R.J. Eanes, and B.D. Tapley, Center for Space Research, University of Texas at Austin, 3925 West Braker Lane, Suite 200, Austin, TX 78759-5321. (chen@csr.utexas.edu; eanes@csr.utexas.edu; tapley@csr.utexas.edu)

C.R. Wilson, Department of Geological Sciences, University of Texas at Austin, Austin, TX 78712. (clarkw@maestro.geo.utexas.edu)

(Received August 5, 1999; revised February 29, 2000; accepted April 3, 2000.)